RESEARCH/REVIEW ARTICLE

Relation between planimetric and volumetric measurements of permafrost coast erosion: a case study from Herschel Island, western Canadian Arctic

Jaroslav Obu,[1,2,3] Hugues Lantuit,[1,2] Michael Fritz,[1,4] Wayne H. Pollard,[5] Torsten Sachs[6] & Frank Günther[1]

[1] Department of Periglacial Research, Alfred Wegener Institute Helmholtz Centre for Polar and Marine Research, Telegrafenberg A43, DE-14473 Potsdam, Germany
[2] Institute of Earth and Environmental Science, University of Potsdam, Am Neuen Palais 10, DE-14469 Potsdam, Germany
[3] Department of Geosciences, University of Oslo, PO Box 1047, NO-0316 Blindern, Oslo, Norway
[4] Department of Earth Sciences, Utrecht University, Heidelberglaan 2, NL-3584 CS Utrecht, The Netherlands
[5] Department of Geography, McGill University, 805 Sherbrooke Street West, Montreal, Canada
[6] German Research Centre for Geosciences, Telegrafenberg, DE-14473 Potsdam, Germany

Abstract

Ice-rich permafrost coasts often undergo rapid erosion, which results in land loss and release of considerable amounts of sediment, organic carbon and nutrients, impacting the near-shore ecosystems. Because of the lack of volumetric erosion data, Arctic coastal erosion studies typically report on planimetric erosion. Our aim is to explore the relationship between planimetric and volumetric coastal erosion measurements and to update the coastal erosion rates on Herschel Island in the Canadian Arctic. We used high-resolution digital elevation models to compute sediment release and compare volumetric data to planimetric estimations of coastline movements digitized from satellite imagery. Our results show that volumetric erosion is locally less variable and likely corresponds better with environmental forcing than planimetric erosion. Average sediment release volumes are in the same range as sediment release volumes calculated from coastline movements combined with cliff height. However, the differences between these estimates are significant for small coastal sections. We attribute the differences between planimetric and volumetric coastal erosion measurements to mass wasting, which is abundant along the coasts of Herschel Island. The average recorded coastline retreat on Herschel Island was $0.68\,\mathrm{m\,a^{-1}}$ for the period 2000–2011. Erosion rates increased by more than 50% in comparison with the period 1970–2000, which is in accordance with a recently observed increase along the Alaskan Beaufort Sea. The estimated annual sediment release was $28.2\,\mathrm{m^3\,m^{-1}}$ with resulting fluxes of $590\,\mathrm{kg\,C\,m^{-1}}$ and $104\,\mathrm{kg\,N\,m^{-1}}$.

To access the supplementary material for this article, please see Supplementary files under Article Tools online.

Arctic coastal erosion rates are among the highest measured in the world despite the fact that the erosional processes are limited to the short ice-free season, which lasts three to four months (Aré 1988; Overduin et al. 2014). Local coastal erosion rates in sites with exposed ice-rich permafrost can exceed $20\,\mathrm{m\,a^{-1}}$ (Jones et al. 2009; Günther et al. 2013; Günther et al. 2015). Lantuit,

Overduin et al. (2012) reported an average erosion rate of $0.5\,\mathrm{m\,a^{-1}}$ for the entire Arctic; 3% of the Arctic coastline is retreating faster than $3\,\mathrm{m\,a^{-1}}$. Particularly vulnerable are coasts consisting of unconsolidated ice-rich sediments, which are subject to a combination of mechanical and thermal action by waves (Aré 1988). The projected rise in Arctic air temperatures is expected to result in higher

1

Abbreviations in this article
DEM: digital elevation model
ESRI: Environmental Systems Research Institute
LiDAR: Light Detection and Ranging (remote
  sensing method)

---

sea-surface temperatures and a longer open water season that will likely increase erosion rates (Overeem et al. 2011; Stocker et al. 2013; Günther et al. 2015).

Erosion of permafrost coasts can cause rapid land loss, which can lead to a loss of habitat, natural resources and archaeological sites, and can endanger modern infrastructure and communities (Johnson et al. 2004; Mars & Houseknecht 2007). Jones et al. (2008) used aerial photography to identify cultural and historical sites on the Alaskan Beaufort Sea coast that were threatened or had already been eroded by coastal erosion. According to Mars & Houseknecht (2007), the threat of land loss can be reasonably well resolved based on coastline retreat rate data derived from satellite imagery.

Soils and unconsolidated deposits in the northern circumpolar region store large quantities of soil organic carbon (Hugelius et al. 2014). Considerable proportions of this carbon are released together with other elements by coastal erosion (Rachold et al. 2004). Lateral fluxes of organic carbon and nutrients can change water and environment quality and significantly alter Arctic coastal ecosystems (Ping et al. 2011). Vonk et al. (2012) estimated that approximately two-thirds of the eroded organic carbon in Arctic Siberia escape to the atmosphere as carbon dioxide, suggesting that coastal erosion is also an important source for greenhouse gas release. In order to estimate mass fluxes of sediment, volumetric erosion data are required.

Previous studies of Arctic coastal erosion were mostly based on linear coastline movements (planimetric coastal erosion) and land loss observations, with few studies estimating actual volume losses (volumetric coastal erosion). This shortcoming is mostly due to the absence of high-resolution DEMs for remote polar regions. Recent volumetric erosion studies used stereo-photogrammetrically or LiDAR-derived DEMs (Jones et al. 2013; Günther et al. 2015). Coastal carbon flux calculations were based mainly on the combination of planimetric coastline movement rates and average cliff heights (e.g., Jorgenson & Brown 2005; Ping et al. 2011; Günther et al. 2013) and assumed that coastline retreat correlates with sediment release. The paucity of volumetric data significantly limits the accuracy of estimates for sediment fluxes by erosion. The use of high-resolution DEM data offers new possibilities to address this knowledge gap. The most recent information on coastal erosion for the Canadian Beaufort Sea is from the 2000s (Solomon 2005; Lantuit & Pollard 2008) and, given the recent sea-ice minima, needs updating.

The aim of our study is to explore the relationship between planimetric and volumetric coastal erosion measurements and the corresponding estimates of sediment release rates for Herschel Island. The specific objectives of this study are to (1) quantify rates of planimetric erosion based on coastline positions digitized from satellite imagery; (2) quantify volumetric erosion rates derived from DEM elevation differences used to convert volume change into estimated sediment release based on excess ground ice data and to estimate organic carbon and nitrogen fluxes; (3) explore the relationship between rates of actual sediment release, coastline movement and sediment release calculated from coastline movement rates combined with cliff height; and (4) update the recent coastline movement rates on Herschel Island and compare them to the existing baseline (1970–2000) calculated by Lantuit & Pollard (2008).

Study area

Herschel Island is located a few kilometres off the Yukon Coast (Canada) in the southern Beaufort Sea. The island is situated at 69°34′N and 138°55′W, is 13 × 15 km in size and covers an area of 110 km^2 (Fig. 1). Mean annual temperature is $-9°C$ and daily averages rise above 5°C in July and August (Burn 2012). Yearly precipitation is between 150 and 200 mm. Permafrost is continuous with a mean annual ground temperature of $-8°C$ at the depth of zero annual amplitude and active layer depths ranging between 40 and 60 cm (Burn & Zhang 2009; Obu et al. 2015). Storm events generate high winds from predominantly westerly and north-westerly directions, with a secondary set of storm events coming from the east to southeast (Hudak & Young 2002; Solomon 2005). Storms are frequent in late August and September and can generate significant wave heights of 4 m and higher (Pinchin et al. 1985). Coastal areas of the southern Beaufort Sea are ice-fast for eight or nine months of the year, with complete sea-ice cover from mid-October through June (Solomon 2005). The trend of lengthening open water season around Herschel Island is 1.5 day a^{-1} for the period 1979–2012 (Barnhart et al. 2014). The tidal range of astronomical spring tides is 0.5 m (Solomon 2005). A sea-level rise of approximately 4 mm a^{-1} has been documented along Arctic coastlines since 1995 (Henry et al. 2012).

Sea-bed topography, sediment structures and ground ice origin suggest that Herschel Island is a push moraine that was formed by the Laurentide Ice Sheet progression (Mackay 1959; Bouchard 1974; Fritz et al. 2012).
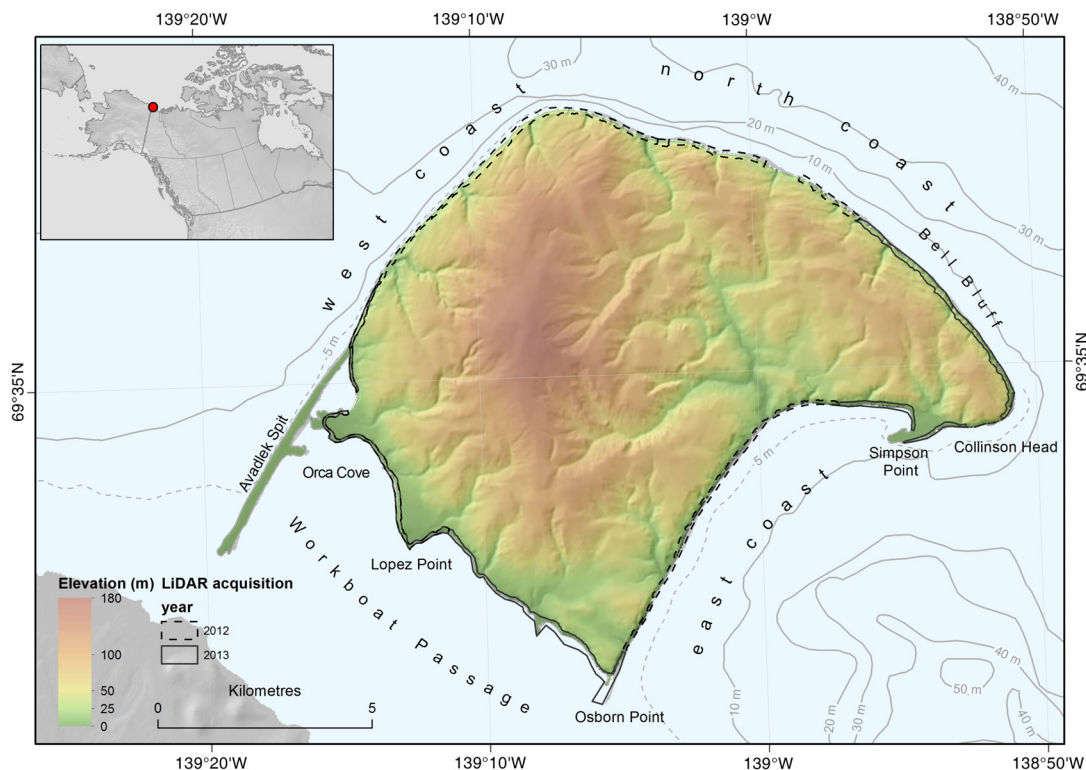
Fig. 1 Hypsometric tint and bathymetry map of Herschel Island in the Canadian Arctic with place names. Coastal areas are marked with the year of the LiDAR DEM acquisition used for calculations. Displayed are also four coastal units (east, north and west coast and Workboat Passage).

The island is therefore made of unconsolidated and mostly fine-grained marine sediment, which contains massive ground ice of glacial and intrasedimental origin (Bouchard 1974; Pollard 1990; Fritz et al. 2011). Herschel Island rises to a maximum height of 180 m a.s.l.; its terrain is diverse and characterized by numerous valleys and gullies, steep coasts and thermokarst phenomena (Lantuit & Pollard 2005, 2008). Mean soil organic carbon and total nitrogen storage for the uppermost 1 m on Herschel Island are estimated to be 34.8 kg C m^{-2} and 3.4 kg N m^{-2} (Obu et al. 2015).

Steep cliffs undergoing erosion and mass wasting processes are prevalent on the Herschel Island coasts (Lantuit & Pollard 2008). Mass wasting may proceed in a cascade-like manner where the slope undergoes several stages from undercutting to levelling. The most rapid observed mass wasting process is block failure, where large blocks are detached from cliffs as a result of undercutting by coastal erosion (Hoque & Pollard 2009). Another observed mass wasting process is retrogressive thaw slumping in which an ice-rich headwall retreats backwards and released material is transported to shore by mudflows, forming fan-shaped accumulations (Lantuit & Pollard 2005). Active-layer detachments are also common along the coasts; these are translational landslides of summer-thawed material (Lantuit, Pollard et al. 2012). The highest and steepest cliffs on Herschel Island are found on the north and west coasts. The cliff height gradually increases from 30 to 50 m from Collinson Head towards the northernmost part of the Island and decreases to 30 m from the northern part towards Avadlek Spit at the southwest corner (Fig. 1). The east coast is less steep, with low cliffs ranging between 20 and 30 m high. Cliffs along Workboat Passage are relatively low and gentle, around 10 m high but up to 20 m close to Osborn Point. Accumulation features resulting from longshore drift include three sand/gravel spits, including Simpson and Osborn points and Avadlek Spit. Ground ice contents by ice type were estimated by Couture (2010). The percentage of excess ice is the highest in Workboat Passage (35%) and along the east coast (13%). The estimated excess ice volumes of the north and west coasts are 2 and 5%, respectively.

Methods

Processing of satellite imagery and coastline mapping

Satellite imagery from different points in time was used to determine the coastline positions. An Ikonos satellite
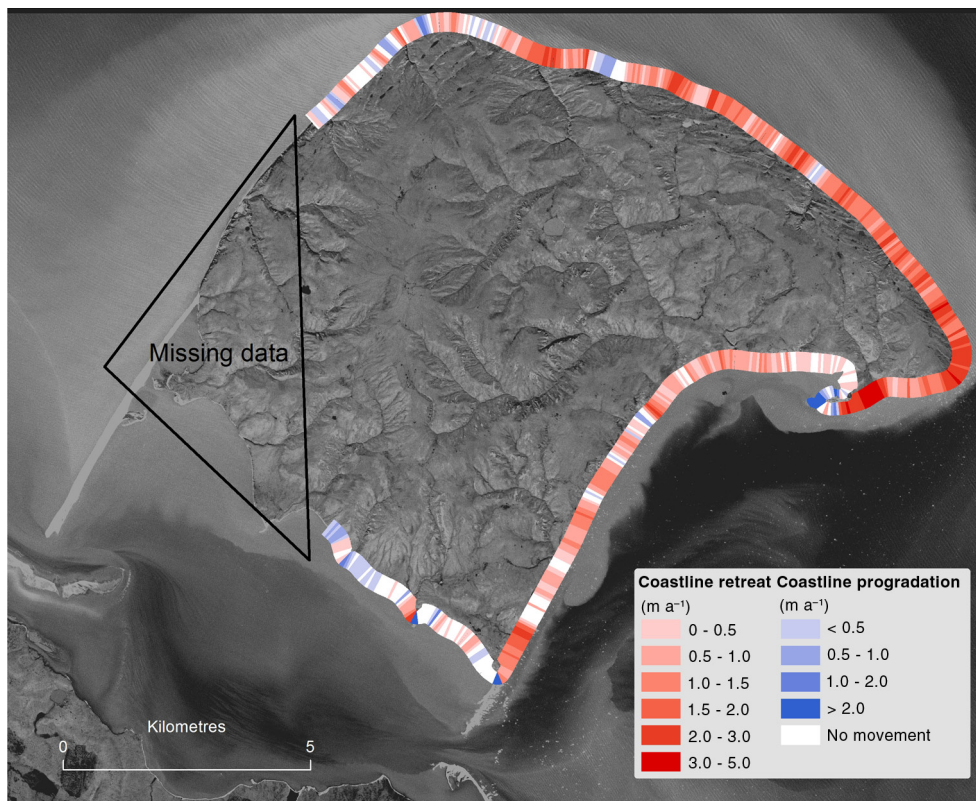
Fig. 2 Map of planimetric erosion inside belt transects on Herschel Island. Net rates of coastline movement in 2000–2011 were calculated from digitized coastlines.

image was acquired on 18 September 2000 and two GeoEye images were acquired on 31 August and 8 September 2011. The raw imagery was processed with Geomatica 2014 Ortho Engine and georeferenced using ground control points collected by Lantuit & Pollard (2008). GeoEye images were mosaicked to 0.5-m pixel spacing, and Ikonos image data were processed to a final 0.6-m pixel spacing. All images were ortho-rectified to mean sea level as the reference plane for a correct coastline position. Residual mean square for the Ikonos image was 0.74 m, and 1.77 m for GeoEye. The Ikonos image did not completely cover the western part of Herschel Island.

We defined the coastline according to Bird (2011: 3) as "the edge of the land at the limit of normal high spring tides." In the case of steep coasts with no accumulations at the shore, the cliff base was mapped, and in the case of low coasts or accumulations, the first beach ridge was mapped. Coastlines were digitized as shapefiles in ESRI ArcGIS 10.3 and used to evaluate planimetric coastal erosion. While the majority of studies on Arctic coastal erosion were based on planimetric erosion, we differentiate coastline movements as both coastline retreat and progradation,

and volume of sediment change (sediment release and accumulation).

DEMs and volume change

High-resolution DEMs from 2004, 2012 and 2013 were used to calculate volumetric changes in the coastal area. The DEM from 2004 is a PhotoSat product created from an Ikonos stereopair from 18 September 2004 with a 2-m pixel spacing and estimated vertical resolution of 0.5 m (Short et al. 2011). DEMs from 2012 and 2013 were acquired from airborne LiDAR scanning that took place during the Airborne Measurements of Methane Fluxes campaigns (Kohnert et al. 2014) on 10 July 2012 and 22 July 2013. Point cloud data were interpolated to raster DEMs with 1-m pixel spacing using an inverse distance weighting algorithm. Vertical accuracy was estimated to be 0.15 m. Obu et al. (2016) described in detail the LiDAR DEM creation procedure. All DEM elevations were referenced to the Earth Gravitational Model 2008 geoid (Pavlis et al. 2008).

DEMs were subtracted to calculate elevation differences. Elevation increase and elevation decrease were
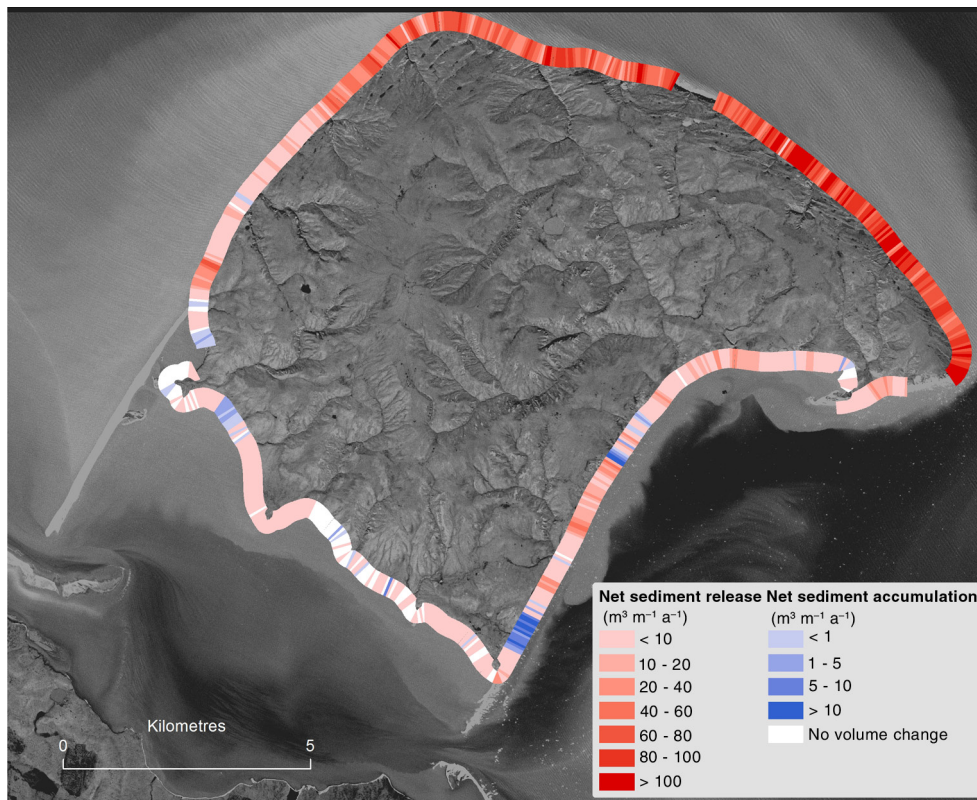
Fig. 3 Map of volumetric erosion inside belt transects on Herschel Island. Net sediment release rates in 2000–2011 are based on DEM elevation changes.
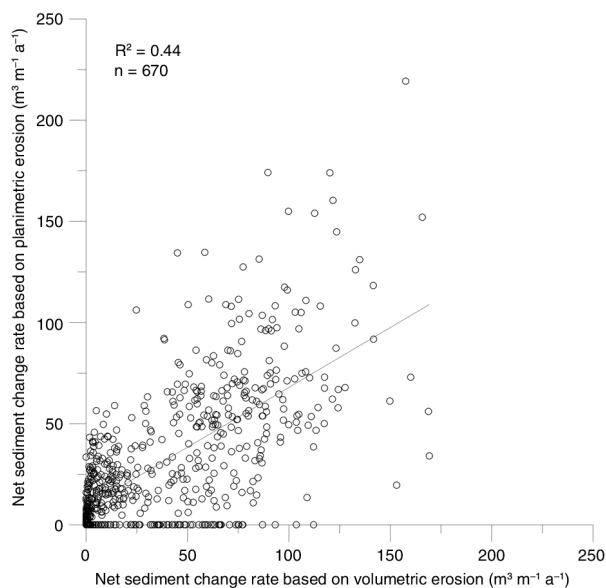
Fig. 4 Scatterplot with linear best fit showing sediment release rates based on DEM elevation change compared to sediment release calculated from coastline retreat and cliff height.

analysed separately. DEM calculations were conducted with ESRI ArcGIS 10.3. Volume change was calculated as the sum of the elevation change multiplied by cell size:

$$V = \sum_{i=1}^{n} A \cdot \Delta h, \qquad (1)$$

where V is the recorded volume change, A is the pixel area and Δh is the elevation difference between two DEM pixels.

In areas of continuous permafrost, ground ice may accumulate far in excess of the pore volume of the same soil in the unfrozen state. The volume of supernatant water present if a vertical column of frozen sediment is thawed is referred to as excess ice (French 2007). The volume of sediment remaining when excess ice has thawed is, therefore, less than the total eroded volume (Aré 1988). Couture (2010) calculated excess ice percentages for different parts of Herschel Island. Released sediment volumes were calculated using the method of Lantuit & Pollard (2005), which took into account the excess ice percentage under the ice-poor overburden material, using the following equation:

$$V_s = \sum_{i=1}^{n} \left[A \cdot (\Delta h - Zo)(1 - \theta) + (A \cdot Zo) \right], \qquad (2)$$
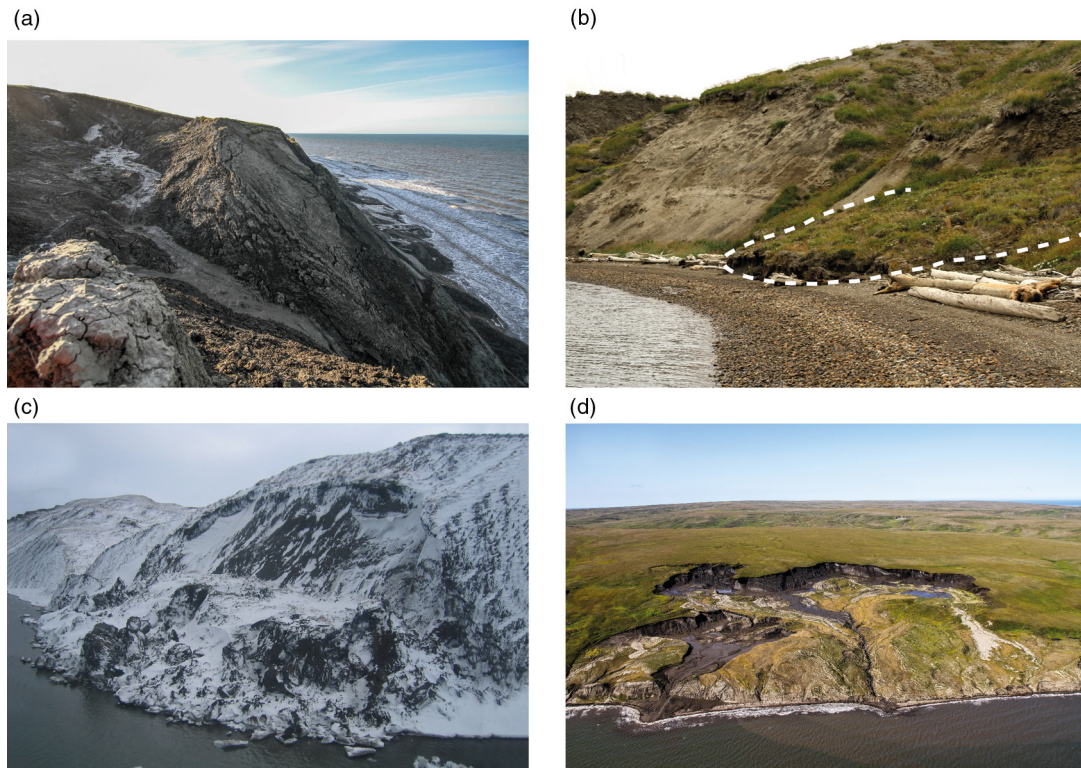
Fig. 5 Coasts of Herschel Island can undergo a series of mass wasting and accumulation processes. Material is transported as mudflows, landslides and block failures before reaching the shore. (a) Slumping, mudflows and shore accumulations on Bell Bluff; (b) active-layer detachment on the east coast (marked with a white dashed line); (c) block failure on the north coast; and (d) retrogressive thaw slump on the east coast.

where V_s is the volume of released sediment, Zo is mean overburden depth and θ is the fraction of excess ground ice. The same authors reported mean overburden material thickness of 1.5 m, which consists of active layer and ice-poor material related to an early Holocene thaw unconformity under the active layer. Volumes were corrected only for erosion (elevation decrease), but not for accumulation (elevation increase), because we assume that after sediment relocation the material is free of excess ice.

Accuracy assessment

Uncertainty in the coastline position can be due to the satellite imagery positioning. Accuracy of coastline position was assessed from the georeferencing uncertainty (δ_r) and the geometric resolution of the data set (δ_p) adapting the method of Günther et al. (2013). The threshold for considered coastline changes was calculated using

$$\delta x = \sqrt{\delta_r^2 + \delta_p^2} \qquad (3)$$

$$\delta cr = \frac{\sqrt{\delta x_1^z + \delta x_2^z}}{t_2 - t_1}, \qquad (4)$$

where δx is the cumulative uncertainty in coastline position, δcr is the change rate uncertainty and t_1 and t_2 are the data set acquisition years. The coastline change rate threshold was 0.18 m a^{-1}.

Elevation change accuracy was estimated using the approach of Jones et al. (2013). Vertical accuracies of the Ikonos-derived and LiDAR DEM data sets were used to calculate the threshold of considered elevation changes:

$$\delta z = 3 \times \sqrt{\delta_{DEM1}^2 + \delta_{DEM2}^2}, \qquad (5)$$

where δz is the elevation change uncertainty and δ_{DEM} is the vertical accuracy of the DEM data sets. The threshold for significant elevation change was 1.57 m.

Coastline movement, sediment release and organic carbon and nitrogen flux estimation

Coastline movements and sediment release were analysed using a series of belt transects, 50 m wide and
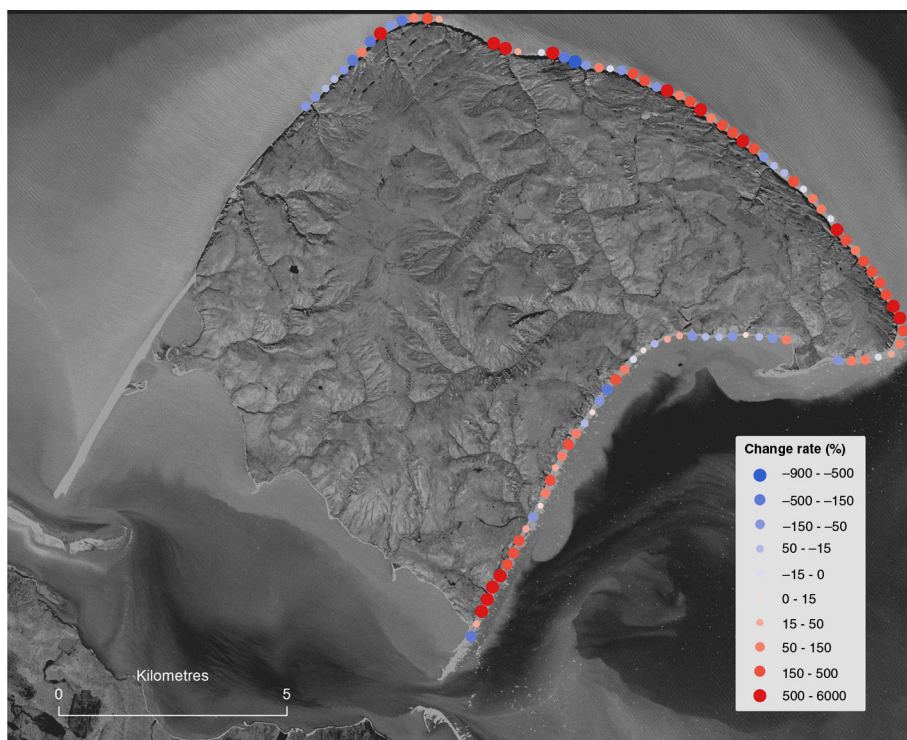
Fig. 6 Rate of change in coastline movement between 1970–2000 and 2000–2011. Coastline movement rates for 1970–2000 were estimated by Lantuit & Pollard (2008).

400 m long (in the inland direction) sections of coast. In total, 963 belt transects were generated for the 48 km of coastline studied. The coast was divided into four coastal units based upon the coastal orientation (Fig. 1).

Coastline movements (planimetric erosion) were analysed along 36 km of coast in the Ikonos and GeoEye image overlap areas. Digitized coastlines were combined to generate polygons, which indicate the coastline retreat or progradation areas. These polygons were clipped by the belt transects to calculate the area of retreat and/or progradation that occurred inside each transect belt. These areas were divided by the belt transect base width (50 m) to get an average coastal retreat or progradation for each belt transect. Average coastline movement for the whole coastline was calculated as total retreat, and progradation area was divided by total studied coastline length. Total retreat distances were divided by the number of years to determine annual retreat rates. Standard deviations were estimated from the rates calculated for the belt transects.

Volumetric erosion was calculated from volume change that was recorded inside the belt transects. Only volume change that was a direct consequence of coastal erosion was considered, including land loss, slumping and mass movements close to the coastline, but not gully erosion and volume changes inside retrogressive thaw slumps in

the hinterland. On account of flight constraints, the swath of the LiDAR surveys did not always cover the whole coastal zone along the track. To achieve the best quality in the volume change data, we included LiDAR data sets from 2012 to 2013 in the volume change analyses and selected the acquisition year according to the best coastal zone coverage (Fig. 1). There were only 3.1 km of coastline with insufficient coverage by both LiDAR DEMs at Bell Bluff, Collinson Head, Simpson Point and Orca Cove. Volume change was also not calculated for Avadlek Spit because the elevation uncertainties were too high. Volume change rates were calculated according to the year of the DEM data set that was chosen for a belt transect.

In order to estimate the sediment released for the entire Herschel Island coastline and four island units (Fig. 1), the sediment release was interpolated for the parts of the island where volumetric erosion data were missing (Bell Bluff, Collinson Head and Orca Cove) as an average of the 20 adjacent transects. Organic carbon and nitrogen fluxes were calculated by multiplying sediment release and carbon and nitrogen storage estimates from Obu et al. (2015) for Herschel Island; they reported storage of 20.9 kg C m^{-3} and 3.7 kg N m^{-3} in the strongly disturbed terrain, which is actively undergoing material removal. This storage reflects the organic carbon and nitrogen

Table 1 Coastline movement, volume decrease, sediment release and carbon and nitrogen fluxes in different coastal units. Volume decrease and sediment release rates include interpolated data for gap filling.

Coastal unit	Mean coastline retreat rate (m a⁻¹)	Mean coastline progradation rate (m a⁻¹)	Mean net coastline movement rate (m a⁻¹)	Mean volume decrease rate (m³ m⁻¹ a⁻¹)	Total volume decrease rate (m³ a⁻¹)	Mean sediment release rate (m³ m⁻¹ a⁻¹)	Total sediment release rate (m³ a⁻¹)	Organic carbon flux (kg C m⁻¹ a⁻¹)	Nitrogen flux (kg N m⁻¹ a⁻¹)	Total organic carbon flux (Tg C a⁻¹)	Total nitrogen flux (Tg N a⁻¹)	Percentage of excess ice (%)
East coast	0.85 ± 0.95	0.19 ± 3.74	-0.66 ± 3.93	6.9 ± 10.8	89000	6.2 ± 9.7	80000	130.1	23.0	1.7	0.30	13.0
North coast	1.22 ± 0.75	0.02 ± 0.10	-1.20 ± 0.79	73.1 ± 30.3	1111000	71.6 ± 29.7	1088000	1495.7	264.8	22.7	4.02	2.6
West coast	0.30 ± 0.42	0.16 ± 0.33	-0.13 ± 0.62	23.6 ± 24.5	189000	23.0 ± 23.9	185000	480.4	85.0	3.9	0.68	4.5
Workboat Passage	0.16 ± 0.35	0.72 ± 0.77	0.56 ± 0.84	1.1 ± 3.1	13000	0.9 ± 2.6	11000	19.3	3.4	0.2	0.04	35.0
Herschel Island	0.88 ± 0.86	0.20 ± 2.26	-0.68 ± 2.48	29.0 ± 37.2	1404000	28.2 ± 36.2	1364000	589.8	104.4	28.5	5.05	/

contents of the parent material that is being eroded at the cliffs.

Sediment release was also calculated using planimetric erosion rates and compared with sediment release calculated from DEMs. The coastline retreat rates were combined with cliff heights, which is an established method for calculating organic carbon fluxes (Lantuit et al. 2009; Ping et al. 2011). We used the following equation:

$$V_{sc} = R \cdot l_t (h - Zo)(1 - \theta) + (R \cdot l_t \cdot Zo), \qquad (6)$$

where V_{sc} is the volume of sediment release estimated from the planimetric retreat rates, h is the cliff height, R is the coastline retreat rate and l_t is the transect width. This equation takes into account the ground ice content and overburden thickness in the same way as does Eqn. 2. Mean cliff height of each transect belt was averaged from DEM elevations.

Update of coastline retreat rates

Lantuit & Pollard (2008) calculated erosion rates on Herschel Island for two periods (1952–1970 and 1970–2000). To estimate the recent change in coastal erosion rates, we updated the rates for the period 2000–2011 using the same survey points. Coastline movement was measured as the distance between the coastline digitized by Lantuit & Pollard (2008) and the coastline digitized in this study.

Results

Planimetric erosion measurements

Net annual rate of coastline retreat along the analysed 36 km of Herschel Island coast in 2000–2011 was 0.68 ± 2.48 m a⁻¹ (Table 1). Average annual coastline retreat rate was 0.88 m a⁻¹, and the average coastline progradation rate was 0.20 m a⁻¹. The percentage of analysed coastline that underwent retreat was 72% and coastline aggradation was 11%. The rest of the coastline did not experience any net change. The highest retreat rate of 5.2 m a⁻¹ was recorded at a low cliff at Simpson Point (Fig. 2). Belt transects with coastline retreat rates from 0 to 0.5 m a⁻¹ were the most common and their frequency gradually decreased towards higher retreat rates (Supplementary Fig. S1a). Coastline retreat rates above 3 m a⁻¹ occurred at the Simpson Point alluvial fan and at Collinson Head.

Coastline retreat rates were the highest along the north coast (Table 1, Fig. 2). They were considerably lower at the west and east coasts and were lowest in the Workboat Passage unit. Coastline progradation occurred sporadically and was most common in Workboat Passage.

Coastal retreat rates showed high variability within all four Herschel Island units. The analysed spits (Simpson and Osborn points) were characterized by fast accumulation and spit extension that resulted in coastline progradation rates above 20 m a^{-1}. Coastline movement rates were not estimated for the part of Workboat Passage and the west coast where coastline movement rates are lower (Lantuit & Pollard 2008). We therefore assume that the average coastline retreat would be slightly lower when including the missing section of coastline.

Volumetric erosion measurements and organic carbon and nitrogen fluxes

Along the entire coastline, the average volume decrease calculated with Eqns. 1 and 2 was 29.0 m^3 m^{-1} a^{-1}, and the resulting sediment release was 28.2 m^3 m^{-1} a^{-1} (Table 1). In contrast to coastline movement, the sediment release showed less variability within the four units. Sediment release rates were high in the whole northern part of Herschel Island (Fig. 3) and were considerably lower along the east and west coasts. The lowest sediment release was recorded in Workboat Passage. The annual net sediment release for the entire island was 1 364 000 m^3 a^{-1}. The resulting organic carbon and nitrogen fluxes were 590 kg C m^{-1} a^{-1} and 104 kg N m^{-1} a^{-1} (Table 1). Sediment release rates showed a bimodal frequency distribution. The most frequent rate was between 0 and 10 m^3 m^{-1} a^{-1}, while a second, less pronounced frequency peak occurred between 60 and 70 m^3 m^{-1} a^{-1} (Supplementary Fig. S1b).

The average sediment release rate based on planimetric erosion that was calculated from planimetric coastline retreat rates and cliff heights (Eqn. 6) was 31.3 m^3 m^{-1} a^{-1}. Calculations based on DEMs for the same transect belts (only overlapping data) gave an average sediment release rate of 35.7 m^3 m^{-1} a^{-1}. This comparison shows that the method using planimetric coastline retreat rates underestimated the average sediment release rate. Although both average release rates are similar, the estimates vary significantly among belt transects. The correlation between both rates inside belt transects is statistically significant ($p < 2.2e^{-16}$) but low (Fig. 4).

Relation between planimetric and volumetric erosion measurements

Estimated planimetric erosion over 11 years (2000–2011) and volumetric erosion over a period of eight to nine years (2004–2012, 2013) overlap for seven years, which is 54 to 58% of the studied time span. The majority of transects that experienced coastline retreat also underwent sediment release. There are also many transects that underwent coastline progradation (negative planimetric erosion) but experienced sediment release (volumetric erosion). Few transects were subject to both coastline progradation and sediment accumulation or coastline progradation and sediment release.

Volumetric erosion and its variability increase with the increase in planimetric erosion rate (Supplementary Fig. S2). High sediment release occurred mostly in transects with a maximum cliff height above 30 m (Supplementary Fig. S3). Volume decrease is also prevalent in transects where coastlines prograded. Considerable sediment release and coastline progradation were recorded together where cliff heights were above 40 m. The highest coastline retreat (>3 m a^{-1}) was accompanied by relatively low sediment release in transects with low cliffs (below 20 m).

Update of coastline retreat rates (2000–2011)

A coastline retreat rate of 0.92 m a^{-1} was calculated for the period 2000–2011 using the same method and transects previously used by Lantuit & Pollard (2008). They reported 0.73 m a^{-1} of annual coastline retreat rate for the period 1952–1970 and 0.54 m a^{-1} for 1970–2000. The coastline retreat rate increased from 1970–2000 to 2000–2011 by 0.38 m a^{-1} and the increase was statistically significant ($P = 0.001$). The correlation between individual coastline movement rates from 1970–2000 and 2000–2011 was very low with ($R^2 = 0.0027$) and values show scattered distribution (Supplementary Fig. S4). The majority of compared coastline transects showed a recent increase in the rate of coastal erosion. None of the transects was characterized by coastline progradation during both analysed periods. Retreat rates have increased at Collinson Head, Bell Bluff and the southern part of the east coast. The increase was mostly recorded in the areas where Lantuit & Pollard (2008) recorded a decreasing retreat rate.

Discussion

Planimetric erosion measurements

We recorded an average coastline retreat rate of 0.68 m a^{-1}, which is similar in magnitude to the rates that were reported for the Beaufort–Mackenzie region (Solomon 2005). Compared to modern coastal erosion rates reported from low-lying coasts along the Dmitry Laptev Strait (Günther et al. 2013) or from the coastal lowlands with ice-rich cliffs of the Alaskan Beaufort Sea coast (Jones et al. 2009), erosion rates on Herschel Island

are low. However, they are comparable to the results of Lantuit et al. (2011) for high cliff coasts on the Bykovsky Peninsula, where the material removal and sediment beach dynamics are more similar to those at Herschel Island (Günther et al. 2013).

The high standard deviation in coastline movement is a consequence of high progradation rates measured on spits, where accumulation occurred (Simpson and Osborn points). Excluding transects with spits, the coastline retreat rate would be 0.80 m a^{-1} with 0.95 m of standard deviation. Solomon (2005) and Lantuit et al. (2011) reported high spatial and temporal coastal erosion rate variability for other parts of the Canadian Beaufort Sea and the Laptev Sea. Obu et al. (2016) showed that high variability in short-term coastline movement rates can result from sediment accumulation. Our results suggest that sedimentation on spits can change rapidly and can alter the average coastline retreat by up to 0.10 m a^{-1}.

Volumetric erosion measurements and soil organic carbon and nitrogen fluxes

The volumetric erosion patterns are different than the planimetric erosion patterns. Planimetric erosion measurements show higher variability and alternation between coastline retreat and progradation, whereas volumetric erosion is more uniform (Figs. 2, 3). The latter is characterized by high rates along the north coast, lower rates along the east and west coasts and low rates at Workboat Passage. Both planimetric and volumetric erosion were the highest along the north coast, but volumetric erosion is considerably higher there in comparison with other parts of Herschel Island. The west coast underwent low planimetric erosion, but considerable volumetric erosion because of the high cliffs. In contrast, the east coast underwent a higher planimetric erosion rate than did the west coast, but the volumetric erosion was considerably lower along the east coast. The north and west coasts have the longest fetch and are the most exposed to predominant storm winds, waves and storm surges (Hudak & Young 2002; Atkinson 2005). For this reason, we assume that volumetric erosion measurements correspond better with environmental forcing than do planimetric erosion measurements.

Organic carbon and total nitrogen fluxes on Herschel Island are higher than those reported from other parts of the Beaufort Sea region. Ping et al. (2011) estimated organic carbon fluxes of 73 kg C m^{-1} a^{-1} for the different coastal types of the Alaskan part of the Beaufort Sea coast, which is considerably lower than our estimate for Herschel Island of 590 kg C m^{-1} a^{-1}. We attribute

this difference to considerably lower cliff heights (1.9 m on average) compared to Herschel Island (18 m), because coastline retreat rates and carbon storage are similar in both regions. The estimate for exposed bluff (3.2 m cliff height) organic carbon flux (163 kg C m^{-1} a^{-1}) for the Alaskan coast was in the range of our organic carbon flux estimations for the east coast of Herschel Island. Organic carbon fluxes from different parts of the Laptev Sea varied between 70 and 850 kg C m^{-1} a^{-1} (Günther et al. 2013) and are closer to the range of the fluxes calculated in our study area.

Relation between planimetric and volumetric erosion measurements

Our results suggest that the relationship between planimetric and volumetric coastal erosion measurements is complex and nonlinear. Rates of volumetric erosion do not necessarily increase with planimetric erosion rates. The average sediment release increases until the coastal retreat rates reach ∼3 m a^{-1}. Further increase in coastal retreat rates results in considerably lower sediment release. Transects with these high retreat rates and low sediment release rates are located along coastal stretches with relatively low cliffs (Radosavljevic et al. 2016), such as the alluvial fan at Simpsons Point. In contrast, high sediment release occurs where the cliffs are higher and coastline retreat rates are not necessarily high. The simultaneous occurrence of sediment release and coastline progradation at high cliffs suggests that these coasts are subject to intermittent transport of material to the shore, where it can cause coastline progradation, despite a net sediment release. The volume increase that occurred together with coastline retreat at some places on the east coast could be explained as a sediment accumulation event that occurred at the coast after 2011, when volume change was recorded by elevation data set, but no coastline movement data were available.

Although the average sediment release estimated from planimetric coastline movement (combined with cliff height) compared to sediment release derived from DEMs is similar, the differences between the same belt transects are significant. The reason is likely the complex relationship between planimetric and volumetric erosion measurements, which is indicated by a low correlation between these estimates (Fig. 4). Elevation classes show weak clustering according to planimetric and volumetric erosion (Supplementary Fig. S3). Lantuit et al. (2009) have shown that sediment releases estimated from coastal erosion rates and cliff height are too uncertain to be a reliable method for Arctic-wide estimation of sediment release. Our study has shown that the same estimations

can also be uncertain on the local scale because of the weak relationship between coastline retreat and sediment release (as in the case of Herschel Island).

We assume that the main reason for nonlinear and complex relationships between coastline movement and sediment release is related to the mass wasting that occurs along the coasts of Herschel Island (Fig. 5). Lantuit & Pollard (2005, 2008) reported numerous active-layer detachments and retrogressive thaw slumps. Obu et al. (2016) demonstrated that slumping can cause significant short-term coastline variations on Herschel Island and along the Yukon Coast. Lantuit, Overduin et al. (2012) and Leibman et al. (2008) indicated that material that is accumulated along the shoreline can inhibit coastal erosion until it is removed from the cliff toe. A constant supply of material to the shore as either sediment or collapsed material likely slows coastline retreat or even causes progradation. For this reason, modelling efforts trying to relate coastal erosion based on coastline movements to different environmental and local factors should consider the effect of material transported to shore by mass wasting. Furthermore, studies that estimate sediment release and carbon fluxes based on coastline movement rates and cliff height should take into account different modes of sediment transport to the coast. The estimates of sediment release based on cliff bottom and cliff top line movements as carried out by Günther et al. (2013) and Kizyakov et al. (2013) can more precisely capture the coastal erosion complexity due to mass wasting.

The relationship between planimetric and volumetric erosion measurements might be less complex in other Arctic coastal environments. In regions with low coasts and high planimetric erosion rates, sediment release estimates based on planimetric erosion would likely be more suitable. An example is erosion observed on coastal sections of Alaska by Jones et al. (2009), where coastal erosion successfully removes the released material. The relationship is probably also more complex on ice-rich coasts with higher elevation, as studied by Hoque & Pollard (2009) and Günther et al. (2013, 2015), where thermoerosional-niche collapses modify simple erosion relationships between planimetric and volumetric erosion measurements. Some of the differences between planimetric and volumetric coastal erosion measurements and consequent sediment release documented in our study might originate from incomplete temporal overlap of our data sets, because several studies have shown a high temporal variability of permafrost coastal erosion (Obu et al. 2016). Increasing availability of high-resolution elevation data sets in the future might offer more opportunities to study volumetric coastal erosion and

sediment release. This would ultimately improve estimates of carbon and nutrient fluxes to the Arctic Ocean and their impact on coastal ecosystems.

Update of coastline retreat rates

We observed an increase of 52% in coastline retreat rates during the period of 2000–2011 in comparison with 1970–2000. Günther et al. (2013) reported a similar increase for East Siberian coasts and Jones et al. (2009) for parts of the Alaskan Beaufort Sea. Jones et al. (2009) attribute this increase to (1) increasing effectiveness of winds from the easterly direction, (2) an increase in open water extent and (3) Arctic Ocean surface warming and sea-level rise. Increased erosion rates on Collinson Head and a decrease in erosion rates on the west coast (Fig. 6) are in accordance with the increasing effectiveness of easterly winds. The general increase of erosion rates on the north coast might be due to increased open water extent (Barnhart et al. 2014) and the later formation of land-fast ice (Mahoney et al. 2014). Scattered values (Supplementary Fig. S4) and the low correlation between the current rates and rates from the 1970–2000 period show that the recent erosion rates have undergone a significant change in spatial patterns. This indicates that the spatial distribution of coastline retreat can vary significantly over time.

Conclusions

Our study has demonstrated a complex relationship between planimetric and volumetric coastal erosion measurements based on observations from Herschel Island. Two important implications are as follows. (1) Spatial patterns of volumetric erosion appear to be less variable than planimetric and correspond better with the exposure of island coasts to wave action. We therefore suggest that volumetric erosion corresponds better with environmental forcing and could provide better coastal erosion modelling results. (2) Sediment release calculated from DEMs on a transect basis shows a low correlation with sediment release calculated from planimetric erosion measurements (combining coastline movement and cliff height). Organic carbon fluxes estimated from DEMs are therefore considerably more accurate. We attribute the complex relationship between planimetric and volumetric measurements of coastal erosion to mass wasting that is occurring on Herschel Island coasts, which is causing temporary coastline progradation while sediment is being continuously removed. As one of the first studies comparing the planimetric and volumetric Arctic coastal erosion measurements, this work can serve as a baseline for further studies that explore this relationship in Arctic

environments, where spatial data availability and field-work possibilities are limited. The observed recent increase in coastal retreat rates on Herschel Island is in agreement with increases observed along the Alaskan Beaufort Sea and the East Siberian Sea coasts.

Acknowledgements

References

Aré F.E. 1988. Thermal abrasion of sea coasts. *Polar Geography and Geology 12*, 2.

Atkinson D.E. 2005. Observed storminess patterns and trends in the circum-Arctic coastal regime. *Geo-Marine Letters 25*, 98–109.

Barnhart K.R., Overeem I. & Anderson R.S. 2014. The effect of changing sea ice on the physical vulnerability of Arctic coasts. *The Cryosphere 8*, 1777–1799.

Bird E. 2011. *Coastal geomorphology: an introduction*. Chichester: Wiley.

Bouchard M. 1974. *Géologie des dépôts meubles de l'île Herschel, Territoire du Yukon*. (Sedimentary geology of Herschel Island, Yukon Territory.) MSc thesis, University of Montreal.

Burn C.R. 2012. *Herschel Island Qikiqtaryuk: a natural and cultural history*. Calgary: University of Calgary Press.

Burn C.R. & Zhang Y. 2009. Permafrost and climate change at Herschel Island (Qikiqtaruq), Yukon Territory, Canada. *Journal of Geophysical Research—Earth Surface 114*, F02001, doi: http://dx.doi.org/10.1029/2008JF001087

Couture N.J. 2010. *Fluxes of soil organic carbon from eroding permafrost coasts, Canadian Beaufort Sea*. PhD thesis, University of Montreal.

French H.M. 2007. *The periglacial environment*. Chichester: Wiley.

Fritz M., Wetterich S., Meyer H., Schirrmeister L., Lantuit H. & Pollard W.H. 2011. Origin and characteristics of massive ground ice on Herschel Island (western Canadian Arctic) as revealed by stable water isotope and hydrochemical signatures. *Permafrost and Periglacial Processes 22*, 26–38.

Fritz M., Wetterich S., Schirrmeister L., Meyer H., Lantuit H., Preusser F. & Pollard W.H. 2012. Eastern Beringia and beyond: late Wisconsinan and Holocene landscape dynamics along the Yukon Coastal Plain, Canada. *Palaeogeography, Palaeoclimatology, Palaeoecology 319–320*, 28–45.

Günther F., Overduin P.P., Sandakov A.V., Grosse G. & Grigoriev M.N. 2013. Short- and long-term thermo-erosion of ice-rich permafrost coasts in the Laptev Sea region. *Biogeosciences 10*, 4297–4318.

Günther F., Overduin P.P., Yakshina I.A., Opel T., Baranskaya A.V. & Grigoriev M.N. 2015. Observing Muostakh disappear: permafrost thaw subsidence and erosion of a ground-ice-rich island in response to Arctic summer warming and sea ice reduction. *The Cryosphere 9*, 151–178.

Henry O., Prandi P., Llovel W., Cazenave A., Jevrejeva S., Stammer D., Meyssignac B. & Koldunov N. 2012. Tide gauge-based sea level variations since 1950 along the Norwegian and Russian coasts of the Arctic Ocean: contribution of the steric and mass components. *Journal of Geophysical Research—Oceans 117*, C06023, doi: http://dx.doi.org/10.1029/2011JC007706

Hoque M.A. & Pollard W.H. 2009. Arctic coastal retreat through block failure. *Canadian Geotechnical Journal 46*, 1103–1115.

Hudak D.R. & Young J.M.C. 2002. Storm climatology of the southern Beaufort Sea. *Atmosphere–Ocean 40*, 145–158.

Hugelius G., Strauss J., Zubrzycki S., Harden J.W., Schuur E., Ping C.-L., Schirrmeister L., Grosse G., Michaelson G.J. & Koven C.D. 2014. Estimated stocks of circumpolar permafrost carbon with quantified uncertainty ranges and identified data gaps. *Biogeosciences 11*, 6573–6593.

Johnson K., Solomon S., Berry D. & Graham P. 2004. Erosion progression and adaptation strategy in a northern coastal community. In M. Phillips et al. (eds.): *ICOP 2003. Permafrost. 8th International Conference on Permafrost. Vol. 1.* Pp. 21–25. Rotterdam: Balkema.

Jones B.M., Arp C.D., Jorgenson M.T., Hinkel K.M., Schmutz J.A. & Flint P.L. 2009. Increase in the rate and uniformity of coastline erosion in Arctic Alaska. *Geophysical Research Letters 36*, L03503, doi: http://dx.doi.org/10.1029/2008GL036205

Jones B.M., Hinkel K.M., Arp C.D. & Eisner W.R. 2008. Modern erosion rates and loss of coastal features and sites, Beaufort Sea coastline, Alaska. *Arctic 61*, 361–372.

Jones B.M., Stoker J.M., Gibbs A.E., Grosse G., Romanovsky V.E., Douglas T.A., Kinsman N.E. & Richmond B.M. 2013. Quantifying landscape change in an Arctic coastal lowland using repeat airborne LiDAR. *Environmental Research Letters 8*, 045025, doi: http://dx.doi.org/10.1088/1748-9326/8/4/045025

Jorgenson M.T. & Brown J. 2005. Classification of the Alaskan Beaufort Sea Coast and estimation of carbon and sediment inputs from coastal erosion. *Geo-Marine Letters 25*, 69–80.

Kizyakov A.I., Zimin M.V., Leibman M.O. & Pravikova N.V. 2013. Thermal denudation, thermal abrasion of sea shores, thermocirques. *Kriosfera Zemli 17*, 36–47.

Kohnert K., Serafimovich A., Hartmann J. & Sachs T. 2014. *Airborne measurements of methane fluxes in Alaskan and Canadian tundra with the research aircraft Polar 5. Reports on Polar and Marine Research 673.* Bremerhaven: Alfred Wegener Institute.

Lantuit H., Atkinson D., Overduin P.P., Grigoriev M., Rachold V., Grosse G. & Hubberten H.-W. 2011. Coastal erosion dynamics on the permafrost-dominated Bykovsky Peninsula, north Siberia, 1951–2006. *Polar Research 30*, article no. 7341, doi: http://dx.doi.org/10.3402/polar.v30i0.7341

Lantuit H., Overduin P.P., Couture N., Wetterich S., Aré F., Atkinson D., Brown J., Cherkashov G., Drozdov D. & Forbes D.L. 2012. The Arctic coastal dynamics database: a new classification scheme and statistics on Arctic permafrost coastlines. *Estuaries and Coasts 35*, 383–400.

Lantuit H. & Pollard W.H. 2005. Temporal stereophotogrammetric analysis of retrogressive thaw slumps on Herschel Island, Yukon Territory. *Natural Hazards and Earth System Science 5*, 413–423.

Lantuit H. & Pollard W.H. 2008. Fifty years of coastal erosion and retrogressive thaw slump activity on Herschel Island, southern Beaufort Sea, Yukon Territory, Canada. *Geomorphology 95*, 84–102.

Lantuit H., Pollard W.H., Couture N., Fritz M., Schirrmeister L., Meyer H. & Hubberten H.-W. 2012. Modern and late Holocene retrogressive thaw slump activity on the Yukon coastal plain and Herschel Island, Yukon Territory, Canada. *Permafrost and Periglacial Processes 23*, 39–51.

Lantuit H., Rachold V., Pollard W.H., Steenhuisen F., Ødegård R. & Hubberten H.-W. 2009. Towards a calculation of organic carbon release from erosion of Arctic coasts using non-fractal coastline datasets. *Marine Geology 257*, 1–10.

Leibman M., Gubarkov A., Khomutov A., Kizyaakov A. & Vanshtein B. 2008. Coastal processes at the tabular-ground-ice-bearing area, Yugorsky Peninsula, Russia. In D.L. Kane & K.M. Hinkel (eds.): *Ninth International Conference on Permafrost. Proceedings of the Ninth International Conference on Permafrost. University of Alasks Fairbanks. June 29–July 3, 2008.* Pp. 1037–1042. Fairbanks: Institute of Northern Engineering, University of Alaska.

Mackay J.R. 1959. Glacier ice-thrust features of the Yukon coast. *Geographical Bulletin 13*, 5–21.

Mahoney A.R., Eicken H., Gaylord A.G. & Gens R. 2014. Landfast sea ice extent in the Chukchi and Beaufort seas: the annual cycle and decadal variability. *Cold Regions Science and Technology 103*, 41–56.

Mars J.C. & Houseknecht D.W. 2007. Quantitative remote sensing study indicates doubling of coastal erosion rate in past 50 yr along a segment of the Arctic coast of Alaska. *Geology 35*, 583–586.

Obu J., Lantuit H., Grosse G., Günther F., Sachs T., Helm V. & Fritz M. 2016. Coastal erosion and mass wasting along the Canadian Beaufort Sea based on annual airborne LiDAR elevation data. *Geomorphology*, doi: http://dx.doi.org/10.1016/j.geomorph.2016.02.014

Obu J., Lantuit H., Myers-Smith I., Heim B., Wolter J. & Fritz M. 2015. Effect of terrain characteristics on soil organic carbon and total nitrogen stocks in soils of Herschel Island, Western Canadian Arctic. *Permafrost and Periglacial Processes*, doi: http://dx.doi.org/10.1002/ppp.1881

Overduin P.P., Strzelecki M.C., Grigoriev M.N., Couture N., Lantuit H., St-Hilaire-Gravel D., Günther F. & Wetterich S. 2014. Coastal changes in the Arctic. *Geological Society, London, Special Publications 388*, 103–129.

Overeem I., Anderson R.S., Wobus C.W., Clow G.D., Urban F.E. & Matell N. 2011. Sea ice loss enhances wave action at the Arctic coast. *Geophysical Research Letters 38*, L17503, doi: http://dx.doi.org/10.1029/2011GL048681

Pavlis N.K., Holmes S.A., Kenyon S.C. & Factor J.K. 2008. An earth gravitational model to degree 2160: EGM2008. Paper presented at the European Geosciences Union General Assembly Symposium. 13–18 April, Vienna, Austria.

Pinchin B.M., Nairn R.B. & Philpott K.L. 1985. *Beaufort Sea coastal sediment study: numerical estimation of sediment transport and nearshore profile adjustment at coastal sites in the Canadian Beaufort Sea. Geological Survey of Canada Open-File Report 1259.* Ottawa: Geological Survey of Canada.

Ping C.-L., Michaelson G.J., Guo L., Jorgenson M.T., Kanevskiy M., Shur Y., Dou F. & Liang J. 2011. Soil carbon and material fluxes across the eroding Alaska Beaufort Sea coastline. *Journal of Geophysical Research—Biogeosciences 116*, G02004, doi: http://dx.doi.org/10.1029/2010JG001588

Pollard W.H. 1990. The nature and origin of ground ice in the Herschel Island area, Yukon Territory. In M.M. Burgess et al. (eds.): *Permafrost–Canada: proceedings of the Fifth Canadian Permafrost Conference. Collection Nordicana 54.* Pp. 23–30. Quebec: National Research Council of Canada.

Rachold V., Eicken H., Gordeev V.V., Grigoriev M.N., Hubberten H.-W., Lisitzin A.P., Shevchenko V.P. & Schirrmeister L. 2004. Modern terrigenous organic carbon input to the Arctic Ocean. In R. Stein & R.W. Macdonald (eds.): *The organic carbon cycle in the Arctic Ocean.* Pp. 33–55. Berlin: Springer.

Radosavljevic B., Lantuit H., Pollard W., Overduin P., Couture N., Sachs T., Helm V. & Fritz M. 2016. Erosion and flooding—threats to coastal infrastructure in the Arctic: a case study from Herschel Island, Yukon Territory, Canada. *Estuaries and Coasts 39*, 900–915.

Short N., Brisco B., Couture N., Pollard W., Murnaghan K. & Budkewitsch P. 2011. A comparison of TerraSAR-X, RADARSAT-2 and ALOS-PALSAR interferometry for monitoring permafrost environments, case study from Herschel Island, Canada. *Remote Sensing of Environment 115*, 3491–3506.

Solomon S.M. 2005. Spatial and temporal variability of shoreline change in the Beaufort-Mackenzie region, Northwest Territories, Canada. *Geo-Marine Letters 25*, 127–137.

Stocker T., Qin D., Plattner G.-K., Tignor M., Allen S.K., Boschung J., Nauels A., Xia Y., Bex V. & Midgley P.M. 2013. *Climate change 2013: the physical science basis. Contribution of Working Group I to the fifth assessment report of the Intergovernmental Panel on Climate Change.* Cambridge: Cambridge University Press.

Vonk J.E., Sánchez-García L., van Dongen B.E., Alling V., Kosmach D., Charkin A., Semiletov I.P., Dudarev O.V., Shakhova N. & Roos P. 2012. Activation of old carbon by erosion of coastal and subsea permafrost in Arctic Siberia. *Nature 489*, 137–140.